FRONT RANGE
COMMUNITY COLLEGE

Optimizing Buoyant Airborne Turbines for Maximum Performance in Limited Space

Connor Gagliano, Kevin Karges, Jesse Knott, Onnie Knott, Marquell Lott

Front Range Community College

Larimer Campus

Engineering Department

4616 S. Shields Street

Fort Collins, CO 80526

Primary Contact: cgagliano3@student.cccs.edu

Abstract

Buoyant airborne turbines are an efficient, but underutilized, green energy option. Despite producing significantly more power than similar ground-based wind power generators at a lower cost [1], buoyant airborne turbines currently have minimal placement options. These types of generators pose risks to aircraft and are prohibited in controlled airspace and can be a risk to the public in the event of catastrophic failure. Because of these limitations, making optimal use of the technology is necessary for it to remain relevant. Seeking options to expand the useful features of buoyant airborne turbines, this study looks at atmospheric data to evaluate the possibility of including solar panels to increase energy output. The purpose of this study is to determine the ideal altitude and environmental conditions for placing buoyant airborne turbines, to maximize the electrical output of both the turbines and coexisting photovoltaic technology. The study will send a package containing atmospheric sensors, wind speed sensors, and solar panels angled to maximize sunlight potential to approximately 100,000 feet on a weather balloon. We hope the data will show an ideal range of altitudes that allow for both solar and wind output without sacrificing functionality of the turbines. Successful test results could indicate the potential for expanding the technology included on buoyant airborne turbines even further, making better use of their finite prospects. Preliminary thoughts include weather observation stations and atmospheric scrubbing technology, as it becomes available.

COSGC Undergraduate Space Research Symposium

Introduction

In the search for green energy solutions, buoyant airborne turbines (BAT) have been proposed to combat the challenges faced by ground-based wind energy farms. A major factor affecting the efficiency of wind farms is the inconsistent nature of the wind at ground level. One solution is to harvest wind energy from higher altitudes where there are fewer obstructions resulting in the wind speed being higher and more consistent. While the idea may not be new, the technology is. George Pocock introduced the idea of kite-based energy harvesting in his 1827 book *The Aeropleustic Art.* [2] This was expanded upon in 1935 when Aloys van Gries filed a patent for such a device. [3] In the mid-1970s, Hermann Oberth submitted designs for a wind turbine hoisted by a balloon. [4] History has numerous examples of the thought process, but only recently has the technology become available to make these ideas tangible. Unfortunately, as with any new technology, there are unique challenges to implementing it. This research endeavor aims to identify methods by which BATs can be optimized for efficiency, energy production, and functionality. As technology and legal avenues advance, it can be anticipated that BATs will become more economically appealing. Currently, many models are in a prototype stage of design and are only implemented in remote areas or as part of disaster relief efforts [5]. Making these stations attractive to the public and investors can aid in the evolution of this technology from experimental to deliverable. Because BATs are limited to such restricted space and number of locations, this research aims to add additional technology to the existing BATs in order to maximize the output of each station. The proposed technology includes solar panels and weather monitoring stations with the potential for additional enhancements if the project is successful. Testing will involve sending wind speed sensors, solar panels and an array of atmospheric sensors to an altitude of 100,000 feet on a weather balloon to monitor their output and tolerance in these conditions.

Background

Airborne wind energy systems (AWES) are a technological solution to harvesting wind energy from higher altitudes and come in many types. Buoyant airborne turbines are a sub-category of AWES. AWES can be broken down into two types: ground-based station (GS) or air-based stations (AS). GS types use a kite or fixed wing aerofoil to turn a generator on the ground. AS types have a generator that is elevated by one of several designs: there is a balloon-lifted type that has a turbine suspended below it, there are some types use electric motors on drones or kites that change from a lift mode to a generator mode once altitude is reached, where the wind holds the kite or drone aloft like a glider, and, finally, there is the type that is hoisted by a blimp with the turbine housed within the center of the blimp. The BAT is this final blimp. [6] The first design for a blimp-style turbine was patented in 1979 by Hermann K. Cymara [7]While, theoretically, [8]Because of these practicalities, technology and the approach to it has been forced to adapt. BATs offer an increased operable range by adding options for obtaining wind

power within realistic parameters. However, much work has yet to be done regarding safety protocols and airspace restrictions before they can be fully utilized. This research proposes that enhancing BAT technology with additional capabilities is an effective stop-gap measure to keep the technology relevant while these obstacles are being addressed.

Process

Buoyant Airborne Turbines are a growing field of research for AWES. After reading an article, *Buoyant Airborne Turbine - The Next Generation of Wind Power,* the team was inspired to determine the optimal altitude for placement of a BAT [5]. The experiment was designed to see if it is possible to expand the mission of a BAT by adding solar panels, a weather station, and carbon capture devices. In order to find the optimal altitude for a BAT several sensors were decided upon as necessary. The primary sensors were to be a wind speed sensor and a pressure sensor. These two sensors would work in conjunction to record where the wind was the strongest. The next sensors chosen were humidity, temperature, and volatile organic compounds (VOC). Humidity and pressure play an important role for wind turbines: higher pressure means more energy is transmitted [9]. The VOC sensor tells us if adding a carbon scrubber would even be a good idea at the altitude. All of these sensors together could be included on a BAT to make a semi-permanent weather station with pollution monitoring. The final sensor to be included is a spectroscopy sensor which, combined with the solar panels that are on the package, will measure how much relative solar radiation is available at various altitudes. Aware that the package may rotate in flight, it was decided to place solar panels and spectroscopy sensors on opposite sides of the package. Knowing this amount of data would overload the Arduino Uno R4 Minima, and with concern for possible in-flight failure of any sensor, it was decided to mount two mirrored Arduinos and double each sensor for redundancy. Finally, having reviewed past COSGC projects that included solar panels that resulted in a lack of usable data, it was observed that the design of those packages were all box shaped packages with side mounted solar panels at a vertical angle. The package was designed to have a pyramidal shape with its top cut off. The sides were positioned at roughly 45 degrees to give the best chance for usable data.

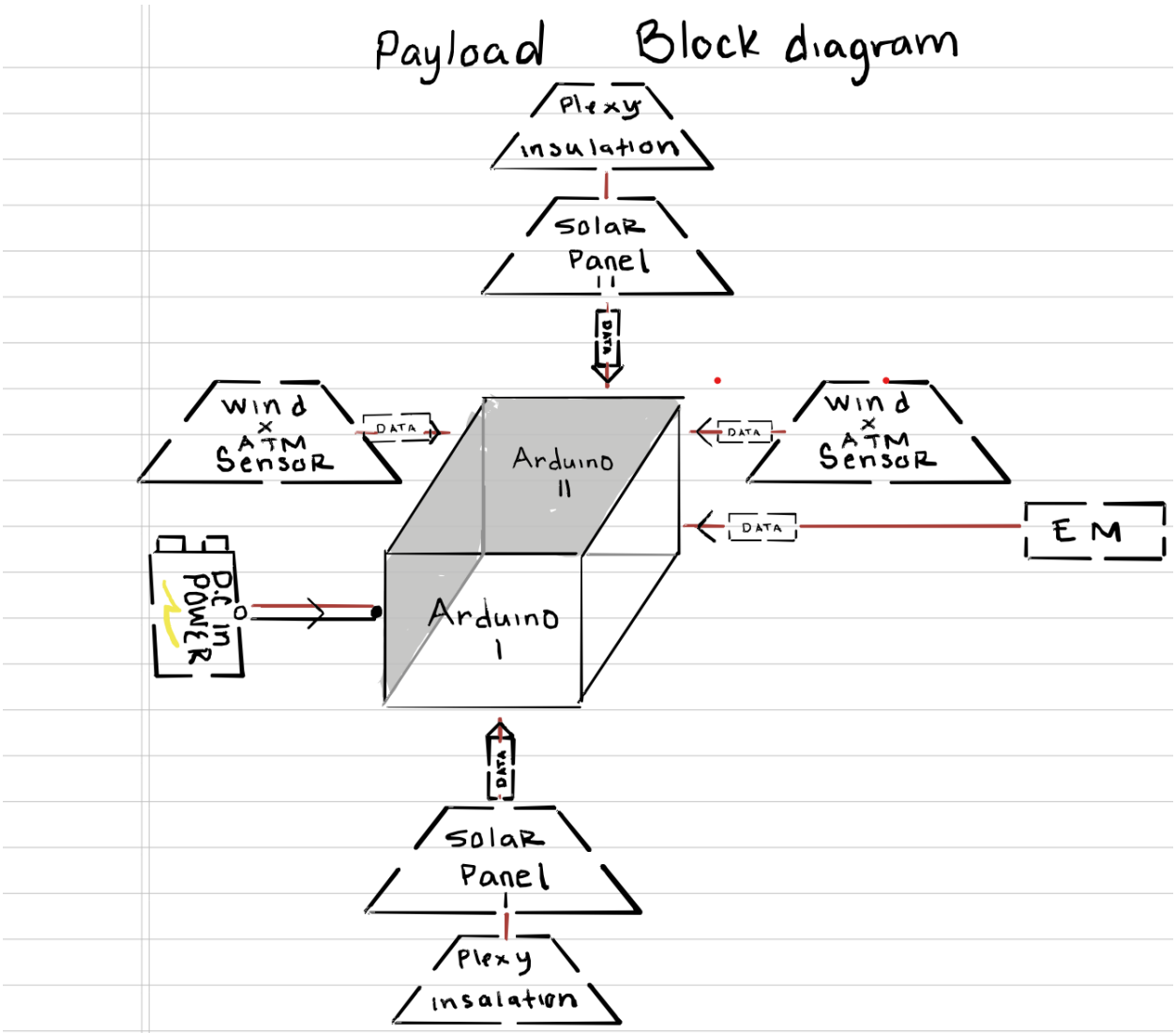

Figure 1: Block diagram

For determining wind speed at altitude, we looked at several options. After much searching, we found the Modern Device Wind Sensor Rev. C which is a hot wire anemometer. It heats up a wire and using the temperature of the wire as the wind blows across it, it then calculates the wind speed. We had to calibrate it to adjust for changing temperature at altitude as well. We also wanted to see if adding solar panels to a BAT would generate more power at higher altitudes, so we included 5V solar panels. To be more precise, in our measurements of solar radiation we included the SparkFun TRIAD spectroscopy sensor which can be connected using QWIIC connect wiring. We also included the QWIIC connect shield from SparkFun as it enabled us to use QWIIC connect wiring. Our final sensor is the Multi-Function Environmental Module CCS811+BME280. We chose this sensor because it encompasses a wide array of sensors in one small chip. The functions of this sensor include temperature, humidity, pressure, and volatile organic compounds (VOC). These sensors fill up the available analog pins on the Minima, but we wanted to get data from all sides of the package since while in flight the package will be

moving. If the solar panels or wind sensors are on the wrong side, they may not get proper data. We thought having two sets of sensors would be ideal. Considering we were at less than half of our weight allotment of 600 grams, we doubled up on Arduinos and sensors and measured the weight of the final package to be 574 grams. Solar panels are usually angled to catch more sunlight and having viewed papers from past projects that used solar panels, we decided to make our package roughly pyramid shaped with a flat top. The solar panels will not be powering the package; they are there to gather solar levels as analog input. To power the Arduinos, we will have two 9V lithium batteries. All of our components are rated to work down to -20 degrees Celsius. But to ensure stability, we added insulation to the entire package. Because the solar panels and spectroscopy sensors need to be attached to the outside of the package, we will be adding plexiglass paneling. The wind sensor and environmental sensor will be slightly protruding from the package to minimize their exposure. The addition of the plexiglass results in a 3% power reduction to the solar panels, which we determined from bench testing with and without the plexiglass. The spectroscopy sensor has roughly the same reduction in signal with the plexiglass. During testing of the code some of the sensors would fail, so we coded in a reset and reboot function when a sensor failed. This ensured data was continuously collected.

Parts and Cost Analysis

Table 1 shows the breakdown of the parts and the total budget for our payload.

Item	Weight	Manufacturer	Quantity	Cost
Arduino Uno Q	20g	Arduino	2	$88.00
9V Batteries	37g	Amazon Basics	1 pack	$31.67
OpenLog	2g	Sparkfun	4	$26.00
SD Card	1g	SanDisk	4	$87.96
Spectroscopy Sensor	6g	Sparkfun	2	$139.90
Solar Panels	20g		5	$15.99
Solar Power Manager	15g	Arduino	4	$32.00
Environmental Sensor	1g	Arduino	2	$60.00
Wind Sensor	1g	Modern Device	2	$43.90

Qwiic Connect Wiring	1g	Sparkfun	2	$20.88
Aluminum tape	?g		1 roll	$6.99
Arduino Uno R4	21g	Arduino	2	$40.00
Qwiic Connect Sheild	15g	Sparkfun	2	$15.50

Budget

$800.00

Total

$608.79

Remaining

$191.21

Results

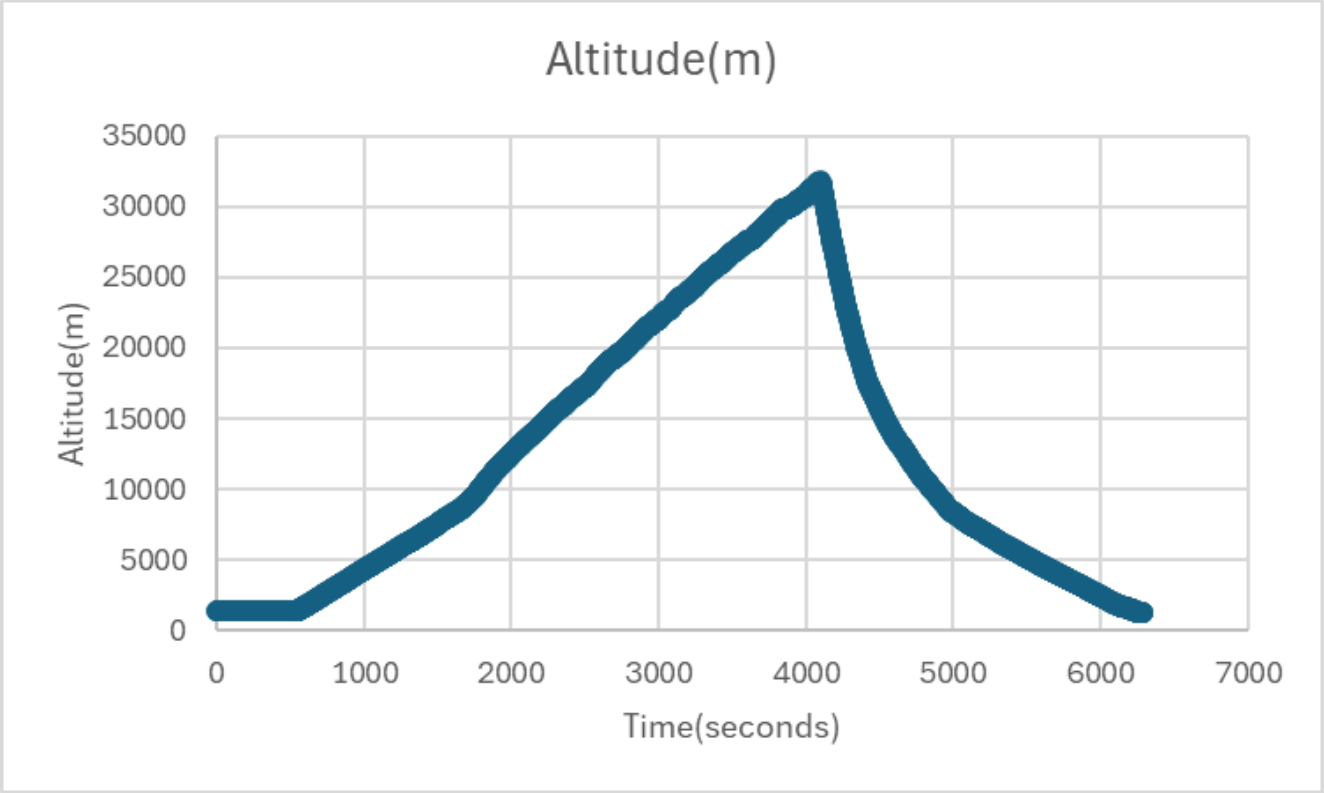

Figure 2: Altitude vs. Time

The altitude versus time plot shows the full vertical profile of the flight from launch through peak altitude and back down to landing. At the beginning of the graph, altitude remains very low for the first several hundred seconds, indicating that the system is still on the ground or ascending very slowly. This initial flat section likely represents pre-launch conditions, or the early phase where lift has not yet significantly increased altitude.

After this point, the graph shows a steady and nearly linear increase in altitude over time. From roughly 1,000 seconds to about 4,000 seconds, altitude increases smoothly from near ground level to a maximum of approximately 31,000 meters. This gradual and consistent climb suggests a stable ascent with minimal interruptions or turbulence strong enough to alter the upward trend. The steady slope of the curve indicates that the vertical speed is relatively constant during this phase.

The peak altitude occurs at around 4,000 seconds (just over an hour into flight), where the graph reaches its highest point. This represents the maximum altitude achieved during the flight. Immediately after reaching this peak, the altitude begins to decrease sharply. The descent phase is noticeably steeper at first, suggesting a relatively rapid loss of altitude shortly after peak

ascent. This could be due to gravitational acceleration combined with reduced lift or deployment of a descent mechanism.

As time continues, the slope of the descent becomes less steep, indicating that the rate of descent slows as altitude decreases. This may reflect increasing air density at lower altitudes, which would create greater drag and gradually reduce the descent speed. Toward the end of the graph, altitude levels off near the ground showing that the system has returned safely and is no longer experiencing significant vertical motion.

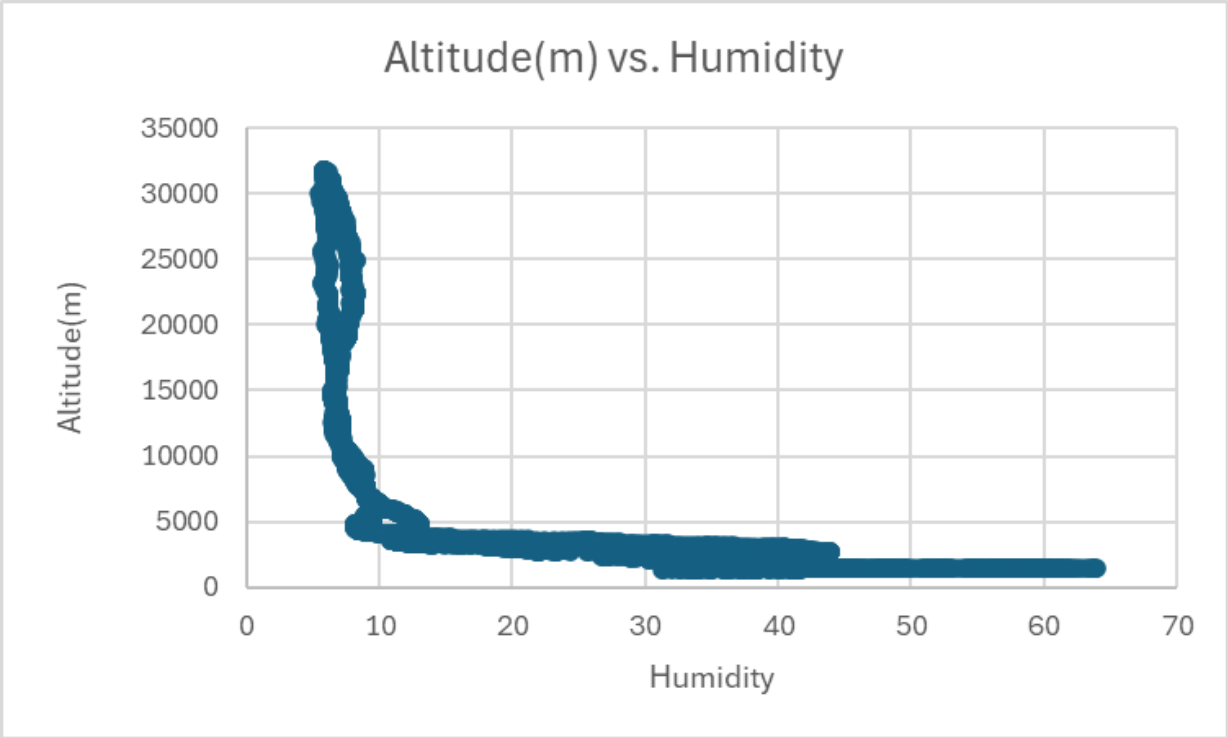

Figure 3: Altitude vs. Humidity

The relative humidity versus altitude graph shows a clear relationship between atmospheric moisture and height above the ground. At lower altitudes, relative humidity values are high, ranging from approximately 30% to over 60%. This clustering near the bottom of the graph indicates that near-surface air contains a larger amount of moisture, which is expected due to evaporation from the ground and vegetation.

As altitude increases, relative humidity decreases sharply. Between about 2,000 and 10,000 meters, humidity drops rapidly to values below 20%. This shows that moisture content diminishes quickly as the system moves upward through the lower atmosphere. The steep decline suggests that most water vapor is concentrated closer to the Earth's surface, where temperatures are higher and the air can hold more moisture.

Above roughly 10,000 meters, the graph shows that humidity remains consistently low, generally under 10%, even as altitude continues to increase toward 30,000 meters. In this region, data points form a vertical cluster with very little horizontal spread, indicating that changes in altitude have minimal impact on humidity at these higher elevations. This suggests extremely dry atmospheric conditions in the upper portions of the flight.

The overall shape of the plot demonstrates a strong inverse relationship between altitude and relative humidity. As altitude increases, relative humidity decreases and then stabilizes at very low values. This trend aligns with known atmospheric behavior, where cooler temperatures and lower pressure at high altitudes reduce the air's ability to retain water vapor.

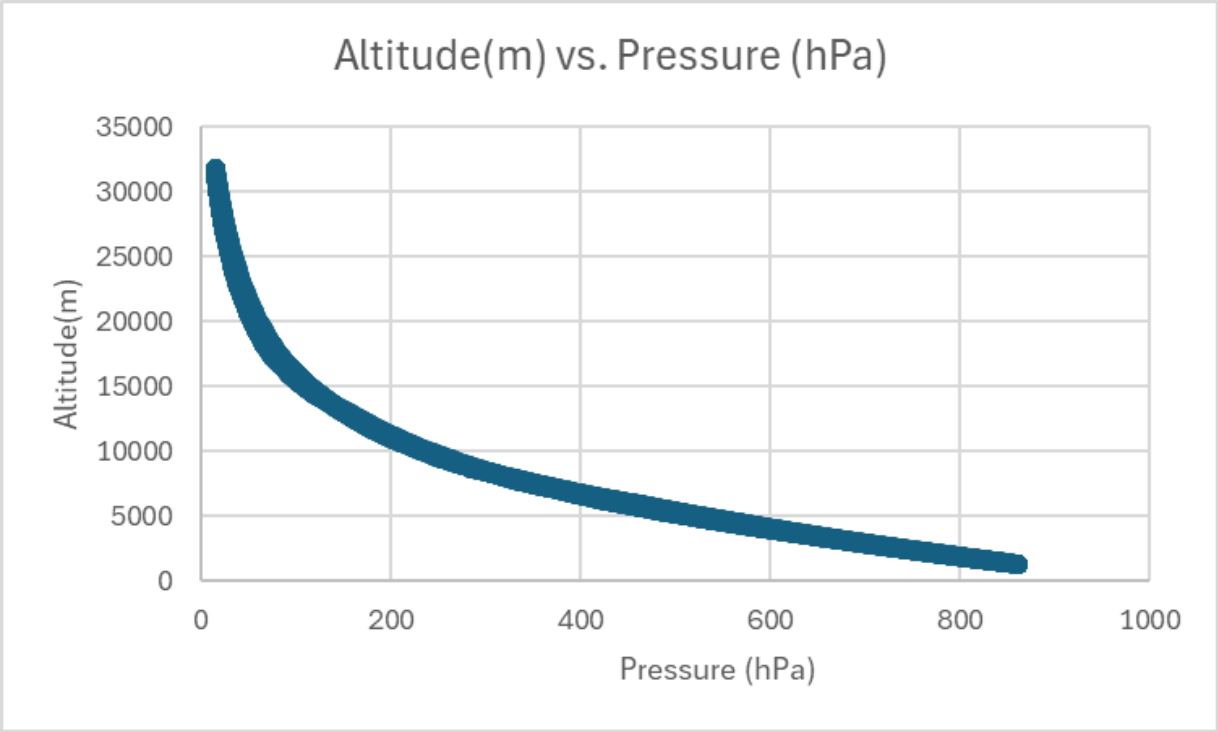

Figure 4: Altitude Vs. Pressure

The pressure vs. altitude graph shows how air pressure changes as altitude increases during the flight. The x-axis shows pressure in hectopascals (hPa), while the y axis shows altitude in meters. Overall, the graph makes it very clear that atmospheric pressure decreases as altitude increases, which is what we would normally expect when moving higher up in the atmosphere.

Near the ground, pressure values are the highest, staying close to the expected Colorado air pressure. In this lower altitude region, the curve is fairly stretched out, meaning that pressure does not drop very quickly at first. This happens because the air near the Earth's surface is much denser, so small changes in altitude do not cause huge changes in pressure right away.

As altitude increases, especially between about 5,000 and 15,000 meters, pressure starts to decrease much more noticeably. The curve begins to bend more steeply, showing that pressure is dropping faster as the system climbs higher. By the time the altitude reaches around 10,000 meters, the pressure has already fallen to a fraction of its original value at the surface. This shows that most of the atmosphere's mass is concentrated at lower altitudes.

At even higher altitudes, above roughly 15,000 meters, the curve becomes very steep. Pressure continues to drop rapidly, reaching very low values near the highest altitudes recorded in the data. In this region, the air is extremely thin, which means there are far fewer air molecules exerting pressure. Small increases in altitude lead to large changes in pressure, which is why the curve looks so sharp toward the top of the graph.

Instead of a straight line, the graph has a curved shape, showing that the relationship between pressure and altitude is not linear. This curved trend reflects how atmospheric pressure depends on the weight of the air above it. As altitude increases, there is less air left above the system, so pressure decreases more and more quickly.

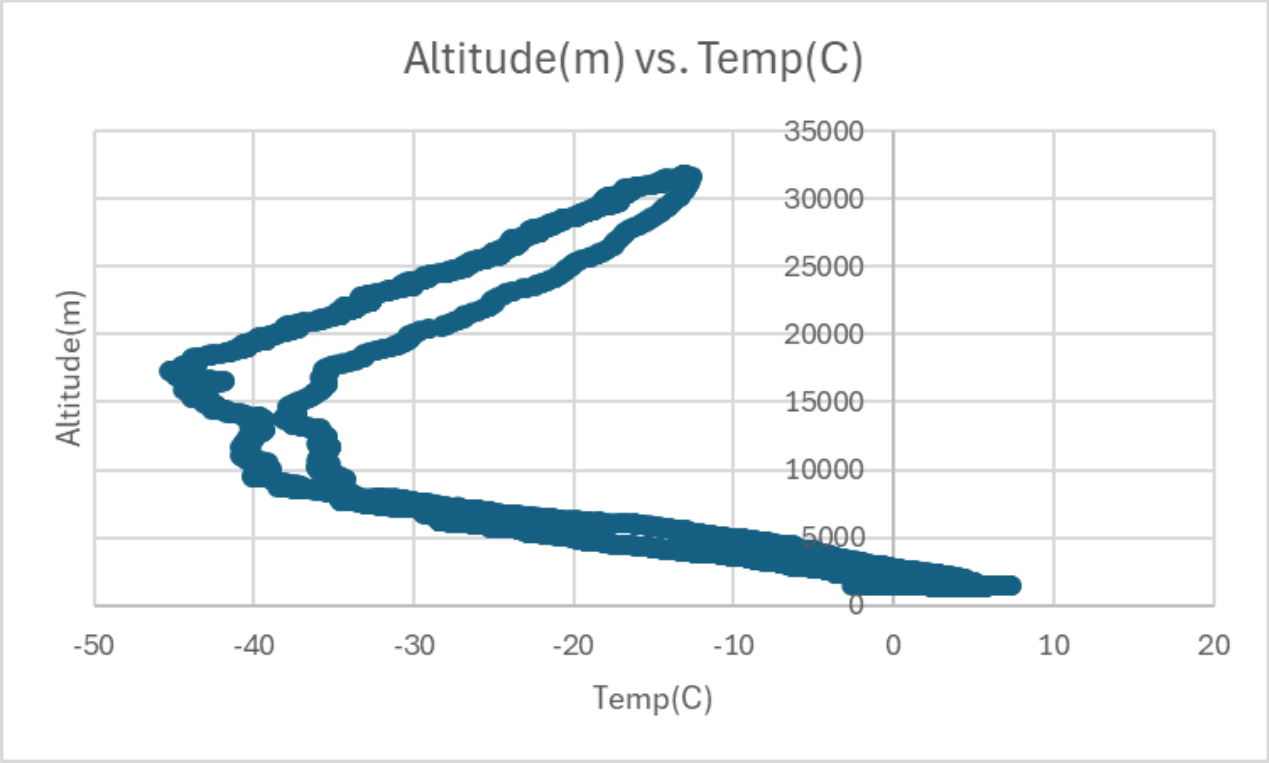

Figure 5: Altitude Vs. Temperature

The altitude versus temperature graph shows how air temperature changes as the system moves higher into the atmosphere. Near the ground, temperatures are the warmest, staying around 0°C. This is expected since air close to the Earth's surface is heated by the ground and nearby surroundings.

As the altitude increases, the temperature drops steadily. Between about 5,000 and 20,000 meters, temperatures fall sharply, reaching lows near –40°C. This shows that the atmosphere gets much colder as elevation increases, which matches what is typically seen in atmospheric data. The curve also forms a loop, showing data collected during both ascent and descent.

At the highest altitudes, around 30,000 meters, temperatures stop decreasing as much and begin to level off slightly. This suggests that the system reached a part of the atmosphere where temperature behavior changes. Overall, the graph clearly shows that temperature decreases with altitude, and the smooth trend suggests that the data collected was consistent and reliable.

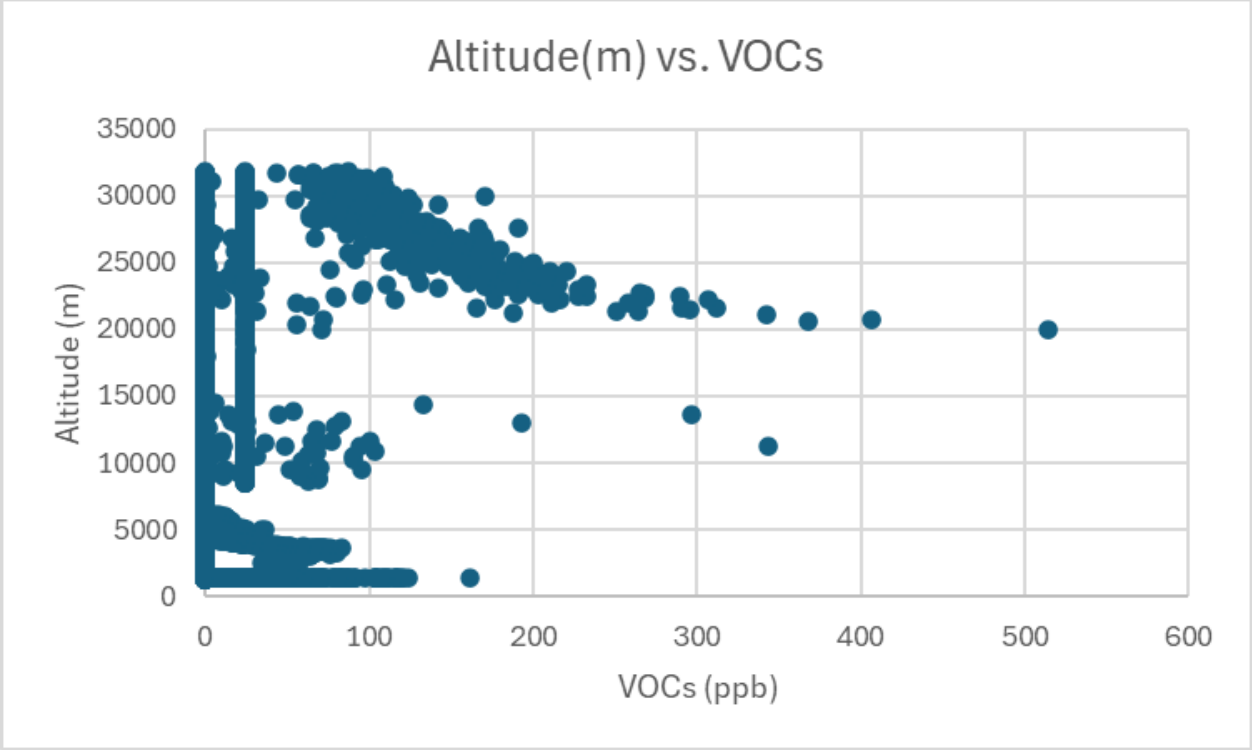

Figure 6: Altitude Vs. Volatile Organic Compounds

Volatile organic compounds (VOCs) max out at about 150 ppb below 2,500 m, showing a steady decrease with altitude approaching 7,500 m. Above 7,500 m there is a spike, ranging under 100ppb but with sporadic readings reaching 350 ppb, up to about 15,000 m where another rapid dip is seen. Above 20,000 m, the largest spike is seen, with the highest reading at 510 ppb, and showing a rapid decline for about 2,500 m before resuming a gradual decline for the remainder of the test. We speculate that the spike in VOC is due to passing through various cloud layers.

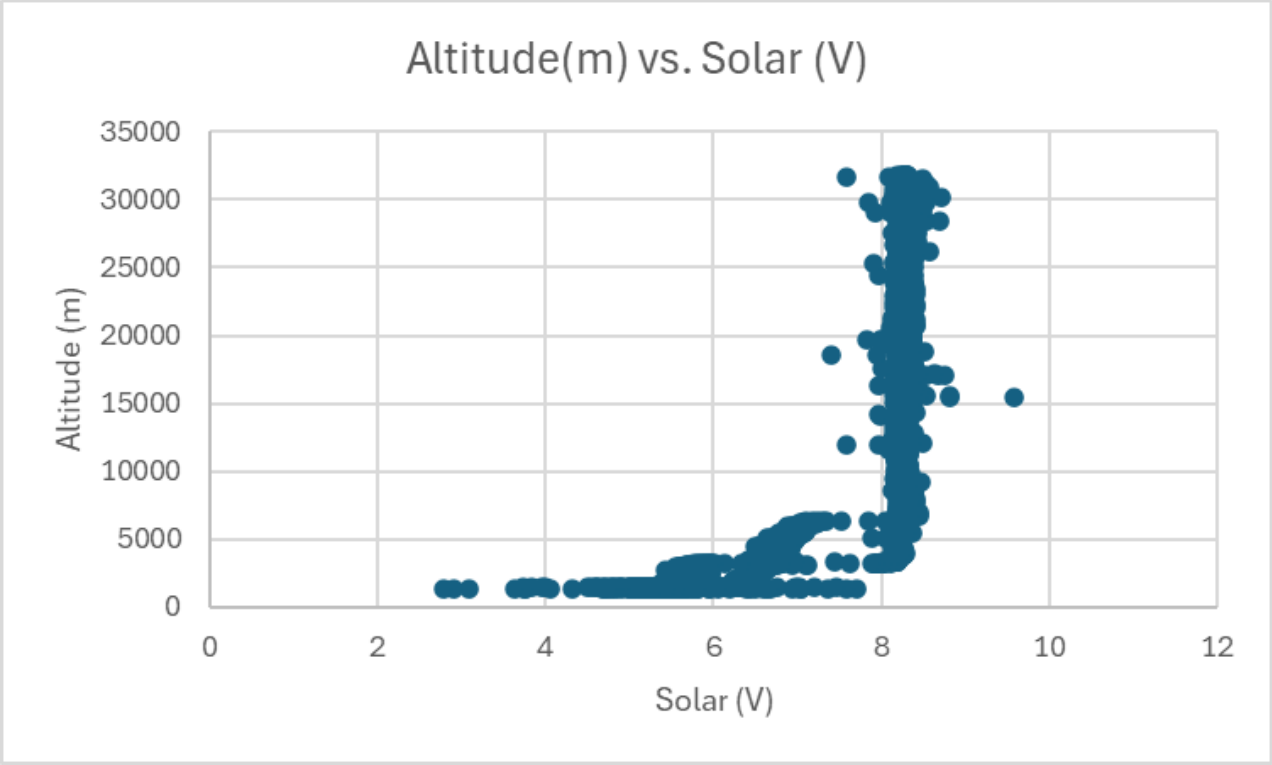

Figure 7: Altitude vs. Solar Voltage Output

The altitude versus solar voltage output graph shows how solar energy production changes as altitude increases. The x axis represents solar voltage output, while the y axis represents altitude in meters. Overall, the graph shows a strong relationship between increasing altitude and increased solar voltage output, especially after the system rises above the lower atmosphere.

At lower altitudes near the ground, solar output values are generally lower, clustering around the mid-range of voltage readings. This is likely due to interference from atmospheric particles, clouds, and shading effects closer to the surface. Near the ground, sunlight has to pass through more air, dust, and moisture, which reduces the amount of energy reaching the solar sensor.

As altitude increases into the mid-range (several thousand meters), solar voltage begins to rise and stabilize. The data points become more tightly grouped, suggesting more consistent solar exposure. This indicates that at these heights, atmospheric interference is reduced, allowing sunlight to reach the sensor more directly.

At higher altitudes, especially above approximately 6,000 meters, solar voltage values are consistently high. The vertical clustering of data points at higher voltage levels shows that solar output remains strong and stable across a wide range of high altitudes. This suggests that once the system reaches thinner air above most cloud layers, solar performance improves significantly and becomes more reliable.

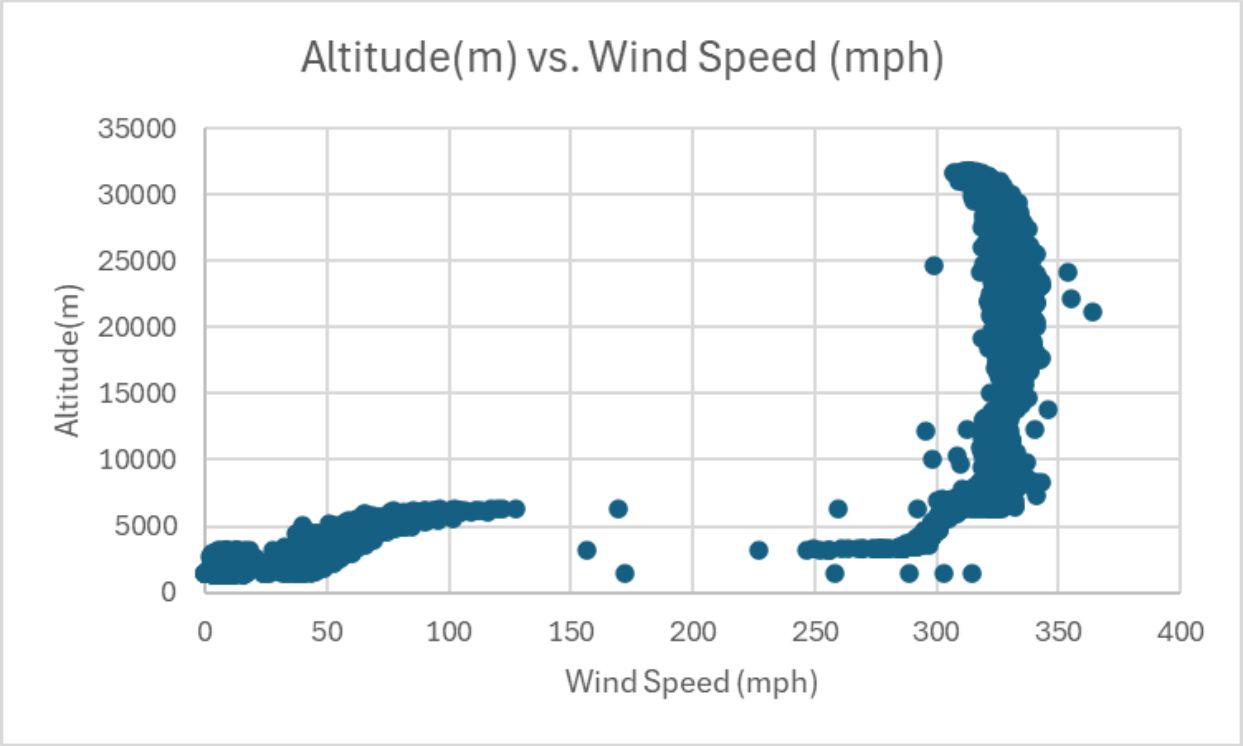

Figure 8: Altitude vs. Wind Speed (mph)

The altitude versus wind speed graph shows how wind speed changes as altitude increases. The x axis represents wind speed, in miles per hour, while the y axis represents altitude in meters. Compared to other charts, this graph shows a dramatic change in behavior between lower and higher altitudes.

At lower altitudes, wind speeds are generally much lower and increase only gradually with height. The data shows a wide cluster of relatively low wind speeds from the ground up to several thousand meters. This is expected, as surface friction from terrain, buildings, and vegetation reduces wind speeds closer to the Earth's surface.

As altitude increases beyond the lower atmosphere, wind speeds increase sharply. At higher altitudes, especially above roughly 15,000 to 20,000 meters, the graph shows very high and consistent wind speeds over 300 mph. The dense vertical clustering at high wind values indicates strong jet stream-like conditions, where air flows much faster due to reduced friction and strong atmospheric pressure gradients.

The sharp curve between lower and higher altitudes highlights a major transition zone in wind behavior. This shows that high altitude environments offer significantly stronger and more reliable wind energy compared to near surface conditions.

Our wind speed data disagrees with known parameters and experiences a sudden, dramatic increase at about 6,000 m, with bursts of high winds throughout. Due to the limitations of the Modern Device Rev C. wind sensor, any data acquired above 60 mph is subject to flaws,

and any data beyond 100 mph can be completely excluded from consideration. At launch, we realized that the idea of obtaining wind speed data from a weather balloon is also flawed, as the balloon moves with the wind, and the wind speed would either be off, or we would be obtaining data from the package rotating. Upon careful consideration, we decided to review other research papers for wind speed data at altitude. It is doubtful that wind speed readings from this test are reliable, and results will be based upon verified atmospheric conditions.

Due to issues with the spectroscopy sensor, we were unable to obtain viable data. Therefore, we will not be able to review the data for discussion.

Discussion

Verifiable research shows that the BAT and other similar devices can operate with wind speeds up to 25m/s or roughly 55 mph. [10] The conditions at 6,000 m correspond to these limitations. The pressure at this altitude has dropped to about 400 hPa, which is roughly half of ground level pressure. This allows for a balance between high wind speeds and lower air pressure resulting in acceptable conditions, if not optimal. The middle cloud layer, containing the bulkiest altostratus and altocumulus clouds, ends at about this altitude [11]. Reason suggests that a lack of cloud cover would offer optimal sunlight, as well as reduced humidity. The data obtained through testing supports this conclusion. VOCs appear to dip at this altitude. However, they reach their highest concentration above the 6,000 m mark. It therefore follows that a carbon scrubber would likely be beneficial for catching VOCs as they rise through the atmosphere. Since the BAT is a semi-permanent fixture, it would be advantageous to include a weather station. This would allow the collection of mid-level atmospheric data on a fixed platform. For the ease of assembly, a modular solar panel system could be adapted to work with the BAT. [12]

Conclusion

Examination of combined atmospheric parameters suggests that an ideal position for an enhanced BAT is between 6,000m and 7,500m. At this altitude solar power is consistent and significant. Humidity is reaching its lowest while air pressure remains within acceptable operating parameters [9]. The temperature at this altitude is moderate compared to the overall range and within tolerance for a weatherized BAT [9]. Wind speeds at this altitude range between 15m/s to 20 m/s [13]. A BAT placed at this altitude could operate successfully, and added solar panels would operate at peak performance. It is likely that atmospheric scrubbers would be effective at this altitude, as they become available. However, our data shows some questions as to whether this is the ideal altitude for their operation. Given that it is speculative technology, it is difficult to be certain, and known technology will be prioritized. A fixed weather station for all high-altitude AWES is recommended.

Appendix A

Components used in the package

Arduino Uno R4

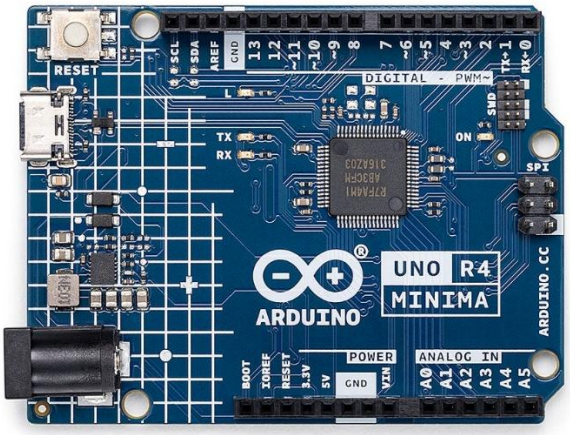

5V Micro Solar Panels

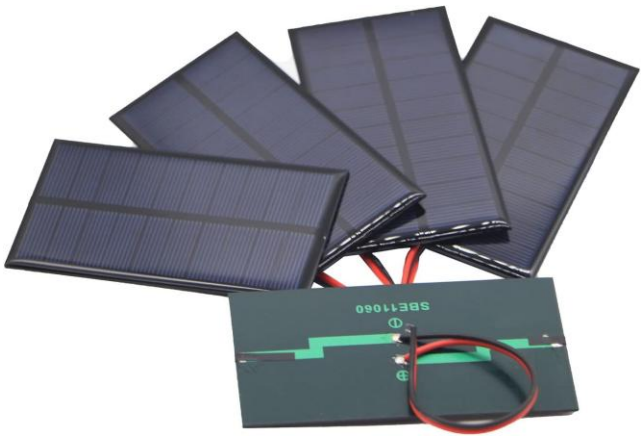

SparkFun Triad Spectroscopy Sensor AS726x

Modern Device Wind Sensor Rev. C

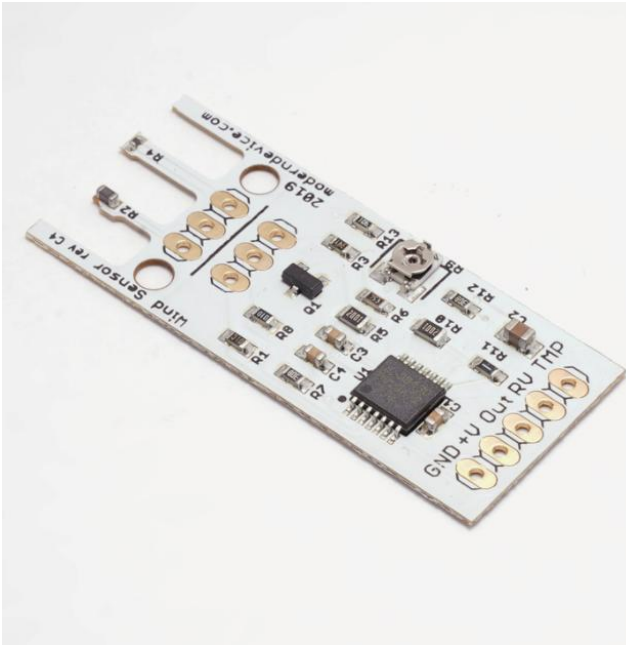

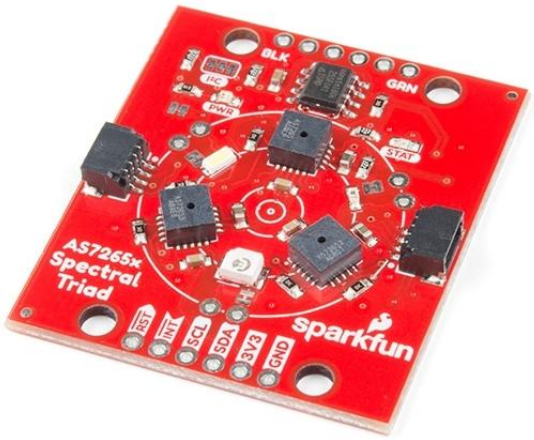

SparkFun Level Shifting microSD Breakout

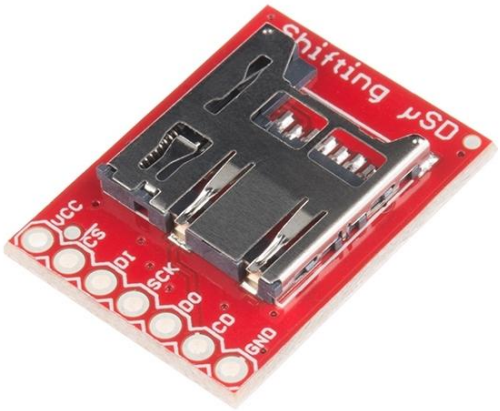

Multi-Function Environmental Module

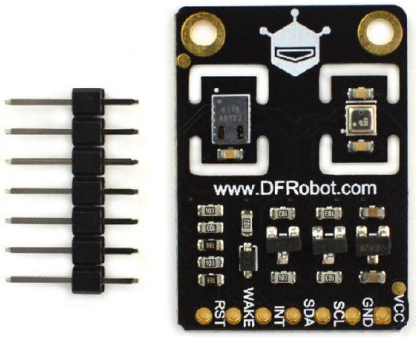

SanDisk Max Endurance micro sd card

Qwiic connect cables

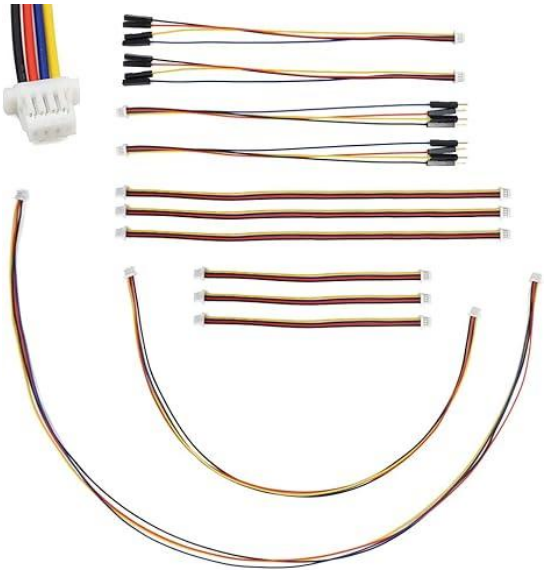

Amazon Basic 9V batteries

V I-Type Battery Connector

SparkFun Qwiic Connect Shield for Arduino

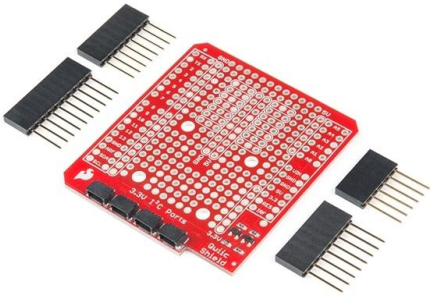

Rocker Switch

Jumper Wires

Aluminum Tape

Foam Board

Bubble insulation

Flight Tube

Paper Clips

Plastic Washer

References

[1] Y. Khurshid, P. Paul, M. Elhesasy, B. Ali, M. M. Kamra, M. Okasha and T. N. Dief, "From inception to commercialization: A systematic review of airborne wind energy systems," *Sustainable Energy Technologies and Assessments,* vol. 83, no. 104623, 2025.

[2] G. Pocock, The Aeropleustic Art, London: Sherwood & Co., 1827.

[3] A. Van Gries, "Wind Power Machine Carried by Kites to Make Use of Altitude Winds". Germany Patent DE656194C, 26 April 1935.

[4] H. Oberth, Primer for Those Who Would Govern, Clarence: West-Art, 1987.

[5] N. Shivani, T. V. Niveditha and K. R. Raghav, "Buoyant Airborne Turbine - The Next Generation of Wind Power," *Journal of Emerging Technologies and Innovative Research,* vol. 6, no. 5, pp. 34-39, 2019.

[6] M. Zou, B. Zhou, B. Wang, J. Chen and H. Luo, "Airborne Wind Energy Systems: Technological Advances and Engineering Challenges," *Carbon Neutral Technologies,* no. 100018, 2026.

[7] H. K. Cymara, "Panemone Wind Turbine". United States Patent US4166596A, 7 November 1979.

[8] C. Jung and D. Schindler, "Distance to Power Grids and Consideration Criteria Reduce Global Wind Energy Potential the Most," *Journal of Cleaner Production,* vol. 317, no. 128472, 2021.

[9] S. H. Danook, K. J. Jassim and A. M. Hussein, "The Impact of Humidity on Performance of Wind Turbine," *Case Studies in Thermal Engineering,* vol. 14, no. 100456, 2019.

[10] A. Saleem and M.-H. Kim, "Performance of Buoyant Shell Horizontal Axis Wind Turbine Under Fluctuating Yaw Angles," *Science Direct,* vol. 169, pp. 79-91, 2019.

[11] National Oceanic and Atmospheric Administration, "The Four Core Types of Clouds," 28 March 2023. [Online]. Available: https://www.noaa.gov/jetstream/clouds/four-core-types-of-clouds. [Accessed 12 April 2026].

[12] A. Majdi, M. D. Alqahtani, A. Almakytah and M. Saleem, "Fundamental Study Related to the Development of Modular Solar Panel for Improved Durability and Repairability," *The Institute of Engineering and Technology Renewable Power Generation,* vol. 15, no. 7, pp. 1382-1396, 2021.

[13] M. Limpinsel, D. Kuo and A. Vijh, "SMARTS Modeling of Solar Spectra at Stratospheric Altitude and Influence on Performance of Selected III-V Solar Cells," in *WCPEC-7*, Waikoloa, 2018.

[14] G. S. Lerchbacher, "Can Buoyancy and Lifting Devices Improve the Performance of Airborne Wind Energy?," DTU Wind & Energy Systems, Roskilde, Denmark, 2024.